MixPrompt: Efficient Mixed Prompting for Multimodal Semantic Segmentation

Zhiwei Hao[1]*, **Zhongyu Xiao**[1]*, **Jianyuan Guo**[2]†, **Li Shen**[3], **Yong Luo**[4], **Han Hu**[1]†, **Dan Zeng**[5]

[1]School of information and Electronics, Beijing Institute of Technology.
[2]Department of Computer Science, City University of Hong Kong.
[3]School of Cyber Science and Technology, Sun Yat-sen University.
[4]School of Computer Science, Wuhan University.
[5]School of Communication and Information Engineering, Shanghai University.

{haozhw, zhongyu.xiao, hhu}@bit.edu.cn, jianyguo@cityu.edu.hk,
mathshenli@gmail.com, luoyong@whu.edu.cn, dzeng@shu.edu.cn

Abstract

Recent advances in multimodal semantic segmentation show that incorporating auxiliary inputs—such as depth or thermal images—can significantly improve performance over single-modality (RGB-only) approaches. However, most existing solutions rely on parallel backbone networks and complex fusion modules, greatly increasing model size and computational demands. Inspired by prompt tuning in large language models, we introduce **MixPrompt**: a prompting-based framework that integrates auxiliary modalities into a pretrained RGB segmentation model without modifying its architecture. MixPrompt uses a lightweight prompting module to extract and fuse information from auxiliary inputs into the main RGB backbone. This module is initialized using the early layers of a pretrained RGB feature extractor, ensuring a strong starting point. At each backbone layer, MixPrompt aligns RGB and auxiliary features in multiple low-rank subspaces, maximizing information use with minimal parameter overhead. An information mixing scheme enables cross-subspace interaction for further performance gains. During training, only the prompting module and segmentation head are updated, keeping the RGB backbone frozen for parameter efficiency. Experiments across NYU Depth V2, SUN-RGBD, MFNet, and DELIVER datasets show that MixPrompt achieves improvements of 4.3, 1.1, 0.4, and 1.1 mIoU, respectively, over two-branch baselines, while using nearly half the parameters. MixPrompt also outperforms recent prompting-based methods under similar compute budgets.The code is available at https://github.com/xiaoshideta/MixPrompt.

1 Introduction

Semantic segmentation assigns a label to each pixel in an image and is a core task in computer vision. Progress in this area has largely been driven by large-scale RGB datasets such as Cityscapes [1] and ADE20K [2]. However, models trained on RGB data alone often struggle in challenging environments, such as low-light or poor weather, where visual cues are weak or missing. To address these limitations, multimodal segmentation approaches integrate data from additional sensors [3, 4, 5, 6, 7, 8, 9, 10, 11, 12, 13]. For example, RGB-D segmentation pairs RGB images with depth information, improving

*These authors contributed equally to this work.
†Corresponding to Han Hu and Jianyuan Guo.

39th Conference on Neural Information Processing Systems (NeurIPS 2025).

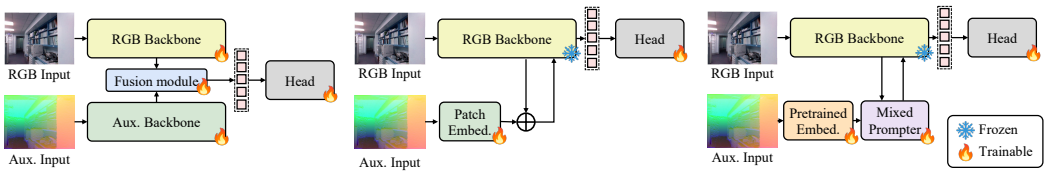

Figure 1: Comparison between (a) conventional multimodal semantic segmentation framework, (b) prompting-based framework, and (c) our mixed prompting framework. Our framework excels by offering superior parameter efficiency while providing a more effective prompting module design.

object separation and spatial understanding [3, 4, 5, 6, 7, 8, 9]. As a result, multimodal methods have surpassed RGB-only models in both accuracy and robustness.

Despite these benefits, two main challenges remain for multimodal segmentation. **First**, model size increases significantly, adding more modalities usually means extra backbone branches and fusion modules [14], which raise computational costs and make deployment difficult on resource-limited platforms. **Second**, multimodal datasets are often much smaller than RGB ones, as collecting aligned data from auxiliary sensors is expensive and labor-intensive. For instance, NYU Depth V2 [15] contains only 1,449 RGB-D pairs, while ADE20K has over 25,000 RGB images. This data scarcity limits both training and generalization.

Recognizing these challenges, we draw inspiration from the vision-language domain [16, 17, 18], where prompt tuning allows a pretrained language model to process visual inputs by introducing visual features as prompts. This method efficiently adapts large models to new tasks or modalities with minimal data and parameters. We extend this idea to semantic segmentation by using a pretrained RGB model as the base, and introducing auxiliary modalities as prompts. Prior work sharing the similar idea [14] simply embeds data from the additional modality directly into the feature space and integrates it with the RGB features through simple addition, treating the modalities as basic addends rather than leveraging their complementary strengths. This method may not fully exploit the potential of the auxiliary modality, potentially leading to suboptimal performance.

To bridge this gap, we propose **MixPrompt**, a mixed prompting framework for efficient multimodal semantic segmentation. MixPrompt embeds auxiliary data using the initial layers of a pretrained RGB extractor, then aligns and fuses features from both modalities at multiple subspaces throughout the backbone. This approach maximizes information transfer with minimal parameter increase. As shown in Figure 1, MixPrompt achieves the efficiency of prompting-based methods while delivering stronger performance. We evaluate MixPrompt on four benchmark datasets: NYU Depth V2 [15], SUN-RGBD [19], MFNet [10], and DELIVER [8]. MixPrompt consistently outperforms strong two-branch and prompting-based baselines, achieving higher accuracy with fewer parameters.

The contributions of our paper can be summarized as follows:

- We introduce MixPrompt, an efficient prompting framework that integrates auxiliary modalities into a pretrained RGB segmentation model, ensuring both data and parameter efficiency.
- We show that reusing early layers of a pretrained RGB backbone is an effective embedding strategy for auxiliary modalities.
- We propose a multi-subspace alignment and prompting strategy that fully leverages auxiliary information, resulting in improved performance over existing baselines.

2 Related works

2.1 Semantic segmentation

Semantic segmentation faces limitations in complex scenarios when relying solely on RGB images, such as low-light conditions and occluded objects. To address these challenges, researchers have introduced multimodal inputs like depth and thermal images. Existing approaches primarily focus on two directions: cross-modal alignment and fusion strategies at various network levels [3, 6, 20, 8, 21, 22, 10, 11, 13, 23], and developing specialized feature extraction architectures for multimodal data [24, 5, 4, 25, 26]. However, these methods often suffer from increased model complexity due to

modality-specific networks and are constrained by the scarcity of large-scale multimodal datasets for pretraining.

2.2 Multimodal prompting

Multimodal prompting has emerged as an effective technique to enhance cross-modal reasoning in vision-language models. Visual prompts, complementing textual prompts, enable pixel-level instructions that help mitigate challenges like visual hallucinations and linguistic biases. Models like CLIP [27] and LLaVA [16] demonstrate how visual prompts combined with large language models can achieve strong performance in multimodal tasks. However, early applications in semantic segmentation, such as Dong *et al.* [14], often fuse multimodal features through simple operations like summation without adequately addressing inter-modal differences, which may interfere with RGB feature distributions and limit visual information capture. The complete literature review, including extensive analysis of prior research and additional references, can be found in the supplementary material (Section A.1).

3 Rethinking Multimodal Prompted Segmentation

Problem setup. Prompt tuning is a technique originally designed to improve the performance of a pretrained language model on a target task without modifying its internal architecture. It involves providing the model with task-specific context through properly constructed prompts. In the field of computer vision, similar ideas have emerged to adapt pretrained models to downstream tasks [28, 29]. A general workflow for this procedure can be formulated as follows:

$$e_i = P_i(h_{i-1}, e_{i-1}), \quad h_i = L_i(h_{i-1}, e_i), \quad y = \text{head}(h_N), \tag{1}$$

where $i \in \{1, 2, \ldots, N\}$ is the layer index. P_i and L_i denote the i-th prompting module and model layer, respectively. h_i represents the output hidden states of layer L_i, and h_0 is the embedded original input. e_i denotes the prompt for layer L_i, while e_0 is the initial prompt at the input stage, which can be either learnable or task-specific parameters. Under this framework, multimodal prompted segmentation can be achieved by using a pretrained single-modality model to extract hidden states from an RGB image, where the prompt e_i is incorporated into the input space at each layer L_i. The initial prompt e_0 is obtained based on the auxiliary modality input, and the intermediate prompt e_i is generated by the prompting module P_i, which takes both the previous hidden state h_{i-1} and prompt e_{i-1} as inputs. Finally, the result of the segmentation y is obtained by processing the hidden state h_N using the prediction head.

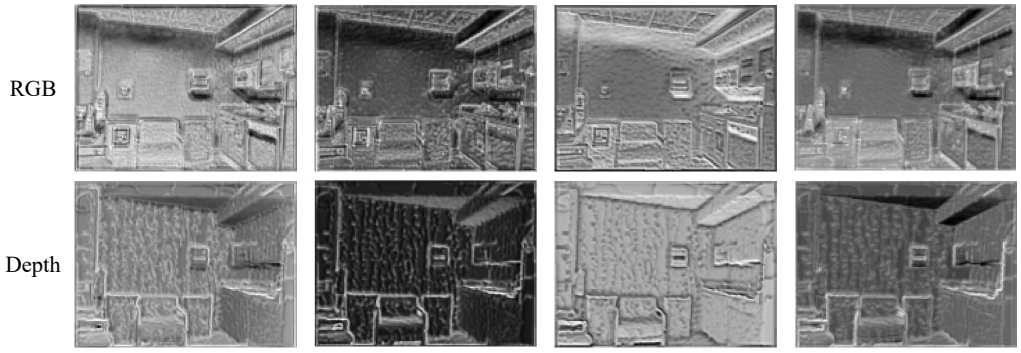

Figure 2: Feature maps extracted from the first stage of a pretrained RGB ResNet50 for RGB and depth inputs, showing that RGB pretrained model can extract meaningful features from depth images.

Rethinking prompt initialization. In the multimodal prompted segmentation framework described above, the way in which auxiliary modality information is introduced into a pretrained model significantly impacts segmentation performance, specifically the initial prompt e_0, as it serves as the entry point for incorporating the auxiliary modality into the model. We reconsider the typical approach to prompt initialization, which often relies on training a new feature extractor specific to the auxiliary modality or using randomly initialized prompts. This random initialization may negatively

affect the final performance of the prompted model. In contrast, we hypothesize that **early layers of a pretrained RGB model could provide a more effective initialization**.

To validate this, we conducted experiments to explore the viability of using pretrained RGB models for initializing the prompt e_0. Specifically, we analyze the feature maps obtained from the first stage of a pretrained ResNet50 model, originally trained on RGB data, using both RGB and depth modality inputs. For this analysis, we use the first sample from the test set of the NYU Depth V2 dataset, which consists of an RGB-depth image pair.

We begin by comparing the feature maps obtained from the model when fed with both RGB and depth inputs. Figure 2 presents a subset of the extracted feature maps for both modalities. These maps show that **both RGB and depth inputs exhibit distinct but rich structural patterns**, with each modality focusing on different aspects of the scene. For instance, the feature maps from the RGB input capture fine edge and texture details, while the depth modality emphasizes depth-related information, such as surface contours and object shapes. Despite the differences in data characteristics, the pretrained RGB model is still capable of extracting meaningful features from the depth modality.

4 Method

4.1 MixPrompt framework

We introduce the MixPrompt framework, a method designed to integrate auxiliary modality information into a pretrained RGB model through efficient and lightweight prompt tuning. As illustrated in Figure 3, our framework utilizes a pretrained RGB model as the backbone for processing RGB images. The auxiliary modality is incorporated via a lightweight prompting module that generates the initial prompt e_0 based on features extracted from the auxiliary input. At each layer i, the backbone layer L_i and the prompting module P_i iteratively fuse and refine features from the hidden state h_{i-1} and the prompt e_{i-1}. The final output is then passed through a segmentation head—initialized with a pretrained RGB segmentation model—to generate the segmentation mask. During training, the backbone remains frozen, as it accounts for the majority of the model parameters. Therefore, only a small subset of parameters is trainable in the MixPrompt framework, ensuring efficient optimization.

The design of prompt initialization stems from our rethinking of how the initial prompt e_0 should be generated. Instead of training an additional modality-specific feature extractor, we propose leveraging the early layers of the pretrained RGB model. These layers are effective for initializing e_0, as they capture general, low-level features that can transfer across different modalities. In the following sections, we will detail the prompting process after obtaining the initial prompt e_0.

4.2 Multi-subspace prompting

We delve into the design of the prompting module in this subsection. In our MixPrompt framework, the prompting module serves as the core, fusing useful information from the auxiliary modality into the backbone. This integration ensures that the final prediction takes the auxiliary modality into account, leading to superior results. However, the features of the main modality in the backbone and those of the auxiliary modality in the prompting branch exist in different feature spaces. Consequently, the prompting module must first align these mismatched feature spaces. Once aligned, the features are fused and fed back into the backbone. This alignment and fusion process relies on two key design principles of our prompting module. The first principle is **parameter-efficient feature alignment**, which ensures that the prompting branch remains lightweight. The second principle is **information-exploitation efficiency** which ensures that we fully utilize the auxiliary information available. The designed prompting module, based on these two principles, is presented at the bottom right of Figure 3.

To achieve parameter-efficient feature alignment, it is essential that the alignment module remains uncomplicated. Therefore, we employ a straightforward linear projection to align the features between the RGB and auxiliary modalities within a low-rank subspace. This approach not only simplifies the alignment process but also enhances computational efficiency by reducing the complexity of the module. Furthermore, the fusion of these aligned features is implemented by simply adding them together, which further promotes efficient computation. This process is formulated as follows:

$$e_i = P_i(h_{i-1}, e_{i-1}) = W_{\text{up}}(W_{\text{rgb}} h_{i-1} + W_{\text{x}} e_{i-1}), \tag{2}$$

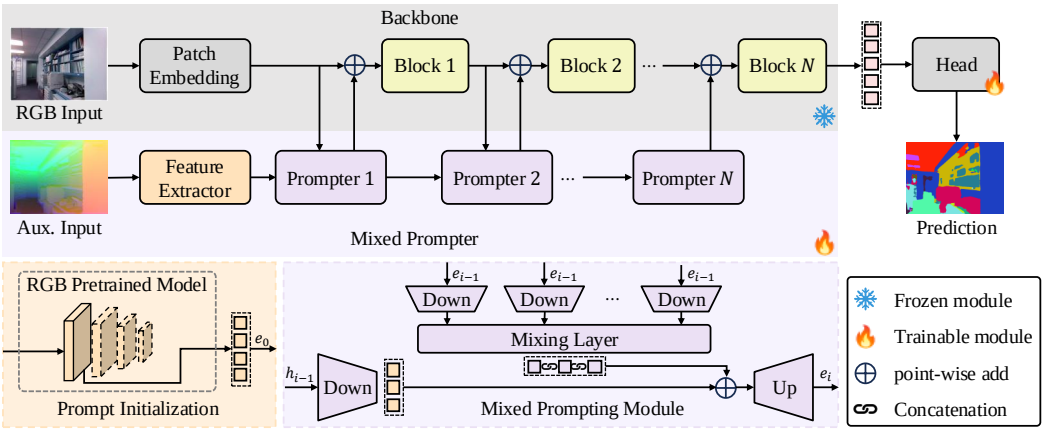

Figure 3: Overall framework of the proposed MixPrompt for multimodal semantic segmentation. The RGB input is processed by an RGB-pretrained segmentation model, while the auxiliary input is processed by a lightweight prompting module. In the prompting module, the initial prompt is derived from the early blocks of the pretrained RGB model (Section 3). At each stage, auxiliary features are projected into multiple subspaces and subsequently mixed to align with the RGB features by mixed prompting modules (Section 4.2). The fused features are used as prompt and is fed back into the main branch. Finally, the segmentation mask is generated by a prediction head based on the output features of the main branch. During training, only the lightweight prompting module and the prediction head are trainable, ensuring the parameter efficiency of the proposed framework.

where $W_{\text{rgb}}, W_{\text{x}} \in \mathbb{R}^{r \times d}$ are down projections and $W_{\text{up}} \in \mathbb{R}^{d \times r}$ is up projection. Here, d is the original feature space, and $r \ll d$ is the dimension of the low-rank alignment subspace. By adopting a small value for r, the prompting module can be made parameter-efficient.

To enhance information-exploitation efficiency, we propose introducing multiple pairs of down and up projections. Each pair aligns the RGB and auxiliary modalities within a distinct subspace, thereby boosting the utilization of useful information. However, this approach increases the number of parameters significantly. Drawing inspiration from the LoRA finetuning method for LLMs [30], we observe that employing an extremely low rank can still yield promising performance. This is because the pretrained LLM operates within a low intrinsic dimension. We make a similar assumption: our pretrained RGB segmentation model also resides in a low intrinsic dimension. Consequently, we reduce the rank of each subspace. This reduction ensures that the overall number of parameters remains unchanged, thereby maintaining parameter efficiency. Taking the RGB features as an example, the projection into multiple subspaces can be represented as:

$$[W_{\text{rgb},1} h_{i-1}, W_{\text{rgb},2} h_{i-1}, ..., W_{\text{rgb},n} h_{i-1}], \tag{3}$$

where $W_{\text{rgb},1}, W_{\text{rgb},2}, ..., W_{\text{rgb},n} \in \mathbb{R}^{\frac{r}{n} \times d}$. n indicates the number of adopted subspaces, where the division of the original rank r by n ensures that the introduction of multiple subspaces does not bring additional parameters. To keep concise, we denote $W_{\text{rgb},n} h_{i-1}$ as h^n_{i-1}. Then, to further improve the representation ability, we introduce a mixing matrix $M \in \mathbb{R}^{n \times n}$ to exchange information between each subspace. The mixed feature $\hat{h}_{i-1}$ becomes:

$$\hat{h}_{i-1} = \left[h^1_{i-1}, h^2_{i-1}, ..., h^n_{i-1}\right] M = \left[\sum_{j=1}^{n} M_{j,1} h^j_{i-1}, ..., \sum_{j=1}^{n} M_{j,n} h^j_{i-1}\right], \tag{4}$$

where $M_{i,j}$ indicates value of the according element in the mixing matrix M. Similarly, we obtain the low-rank representation of the prompt e_{i-1} as $\hat{e}_{i-1}$. The information from the RGB modality is then injected into the low-rank prompt by addition and back-projected into the original feature space via the linear projection $W_{\text{up}} \in \mathbb{R}^{d \times r}$ to yield the new prompt e_i. Once the prompt e_i is obtained, the backbone layer L_i directly fuses the RGB feature with the prompt via addition. The whole process can be formulated as:

$$h_i = L_i(h_{i-1} + W_{\text{up}}(\hat{h}_{i-1} + \hat{e}_{i-1})). \tag{5}$$

The mixed prompting module performs information mixing only between different subspaces of the RGB modality, based on the rationale that mixing information across subspaces on both modalities

Table 1: Comparison of various multi-modal fusion methods on RGB-D segmentation datasets. Results are obtained through multiscale testing. '-' indicates that the corresponding results are not provided in the original paper. '*' denotes the result from the the single-modal version of the method using only RGB input.

Model	Backbone	Params	NYU Depth V2			SUN-RGBD		
			Input size	FLOPs	mIoU	Input size	FLOPs	mIoU
SegFormer* [34]	MiT-B4	62.4M	480×640	74.7G	52.3	530×730	96.3G	49.1
ACNet [3]	ResNet50	116.6M	480×640	126.7G	48.3	530×730	163.9G	48.1
SGNet [4]	ResNet101	64.7M	480×640	108.5G	51.1	530×730	151.5G	48.6
SA-Gate [5]	ResNet101	110.9M	480×640	193.7G	52.4	530×730	250.1G	49.4
GEN [6]	ResNet101	118.2M	480×640	118.2G	51.7	530×730	790.3G	50.2
ShapeConv [24]	ResNext-101	86.8M	480×640	124.6G	51.3	530×730	161.8G	48.6
ESANet [22]	ResNet34	31.2M	480×640	31.2G	50.3	480×640	34.9G	48.2
TokenFusion [21]	MiT-B3	45.9M	480×640	94.4G	54.2	-	-	-
TransD-Fusion [20]	Swin-B	84.0M	480×640	-	55.5	530×730	-	51.9
Omnivore [25]	Swin-B	95.7M	480×640	95.7G	54.0	-	-	-
CMX [7]	MiT-B2	66.6M	480×640	67.6G	54.4	530×730	86.3G	49.7
CMX [7]	MiT-B4	139.9M	480×640	134.3G	56.3	530×730	173.8G	52.1
CMX [7]	MiT-B5	181.1M	480×640	167.8G	56.9	530×730	217.6G	52.4
CMNext [8]	MiT-B4	119.6M	480×640	131.9G	56.9	-	-	-
DFormer [26]	DFormer-L	39.0M	480×640	65.7G	57.2	530×730	83.3G	52.5
DPLNet [14]	MiT-B5	88.58M	480×640	105.0G	59.3	530×730	132.9G	52.8
Ours	MiT-B5	87.2M	480×640	109.0G	**61.2**	530×730	137.9G	**53.5**

could hinder alignment and lead to suboptimal performance. The overall workflow of is presented in the supplementary material (Algorithm 1).

Analysis. The proposed prompting method adopts multiple subspaces for feature fusion, which acts somewhat like the adaptation of a mixture of experts in LLM design [31, 32], where matrix M is the router to assign different importance to each subspace by mixing them with different weights. When $n = 1$ or when all elements in M are equal to $1/n$, the prompting module downgrades to the base architecture in Equation 2. More quantitative analysis in the supplementary material (Section C.5) further validates this design, showing that moderate numbers of subspaces yield optimal performance by enhancing inter-subspace diversity. Another impact of the mixed prompting module comes from reparameterization [33]. While the introduction of multiple subspaces does not involve any non-linear operations, it allows the model to leverage a multi-branch architecture. This modification of the gradient flow helps the model achieve better performance by facilitating more effective information propagation. By aligning features in a low-rank subspace, we adhere to the design principle of parameter-efficient feature alignment. Additionally, the introduction of multi-subspace prompting and the information mixing scheme ensures the principle of information-exploitation efficiency, enabling the final model to achieve effective and efficient multimodal fusion.

5 Experiments

5.1 Experimental Setup

To validate the effectiveness of MixPrompt, we conduct experiments on multiple datasets with RGB and auxiliary modalities, including RGB-Depth, RGB-Thermal, RGB-Event, and RGB-Lidar. NYU Depth V2 [15] dataset contains 1,449 RGB-D samples across 40 categories. SUN-RGBD [19] includes 10,335 RGB-D images with 38 classes. MFNet [10] provides 1,569 RGB-Thermal pairs from 9 classes. DELIVER [8] comprises 3,983 training and 2,005 testing samples with RGB, Depth, Event, and Lidar modalities across 25 categories.

We use the mean Intersection over Union (mIoU) metric for evaluation, with multiscale testing on NYU Depth V2 and SUN-RGBD, and single-scale testing on other datasets, aligning with the evaluation practices of prior works. For the backbone network, we utilize the Mix Transformer encoder (MiT) [34] pretrained on the ADE20K dataset [2]. The auxiliary modalities are projected into the feature space using modules placed before the second stage of a ResNet50 [35] network, which initializes the prompt information. This prompt is then fused across multiple scales using four mixed

Table 2: Comparison of RGB-T segmentation performance on MFNet. Results marked with an underline show the second-best performance in each category, while those in bold indicate the highest score for that class. UL: Unlabeled, PS: Person, CT: Car top, GD: Guardrail, CC: Color cone.

Method	Backbone	Params	FLOPs	UL	Car	PS	Bike	Curve	CT	GD	CC	Bump	mIoU
MFNet [10]	-	-	-	96.9	65.9	58.9	42.9	29.9	9.9	0.0	25.2	27.7	39.7
RTFNet [11]	ResNet152	245.7M	185.2G	98.5	87.4	70.3	62.7	45.3	29.8	0.0	29.1	55.7	53.2
PSTNet [12]	ResNet18	105.8M	123.4G	97.0	76.8	52.6	55.3	29.6	25.1	**15.1**	39.4	45.0	48.4
FuseSeg [13]	DenseNet161	141.5M	193.4G	97.6	87.9	71.7	64.6	44.8	22.7	6.4	46.9	47.9	54.5
U2Fusion [36]	VGG16	-	-	97.7	82.8	64.8	61.0	32.3	20.9	-	45.2	50.2	50.8
AFNet [37]	ResNet50	-	-	98.0	86.0	67.4	62.0	43.0	28.9	4.6	44.9	56.6	54.6
ABMDRNet [38]	ResNet50	64.6M	194.3G	**98.6**	84.8	69.6	60.3	45.1	33.1	5.1	47.4	50.0	54.8
FEANet [39]	ResNet152	337.1M	255.2G	98.3	87.8	71.1	61.1	46.5	22.1	6.6	55.3	48.9	55.3
GMNet [40]	ResNet50	149.8M	153.0G	97.5	86.5	73.1	61.7	44.0	42.3	14.5	48.7	47.4	57.3
TarDAL [41]	-	297M	-	97.6	80.7	67.1	60.1	34.9	10.5	-	38.7	45.5	48.6
EAEFNet [42]	ResNet152	200.4M	147.3G	-	87.6	72.6	63.8	48.6	35.0	14.2	52.4	58.3	58.9
CACFNet [43]	ConvNeXt-B	198.6M	101.4G	-	89.2	69.5	63.3	46.6	32.4	7.9	54.9	58.3	57.8
PAIF [44]	-	260M	-	88.1	72.4	48.1	60.8	-	-	-	**56.0**	57.2	56.5
CENet [23]	ResNet50	-	-	98.1	87.8	71.4	63.2	47.5	31.1	-	48.9	50.3	56.1
SegMiF [45]	MiT-B3	-	-	98.1	87.8	71.4	63.2	47.5	31.1	-	48.9	50.3	56.1
CMX [7]	MiT-B2	66.6M	67.6G	98.3	89.4	74.8	64.7	47.3	30.1	8.1	52.4	59.4	58.2
CMX [7]	MiT-B4	139.9M	134.3G	98.3	90.1	75.2	64.5	50.2	35.3	8.5	54.2	**60.6**	59.7
CMNeXt [8]	MiT-B4	119.6M	131.9G	98.4	**91.5**	**75.3**	**67.6**	**50.5**	40.1	9.3	53.4	52.8	59.9
DPLNet [14]	MiT-B5	88.58M	105.0G	-	-	-	-	-	-	-	-	-	59.3
Ours	MiT-B5	87.2M	109.0G	98.3	90.2	74.5	65.2	50.1	**48.3**	10.5	51.7	52.0	**60.1**

prompting modules, effectively integrating the auxiliary information into the RGB backbone at various levels. Additional optimization details are provided in the supplementary material (Section C.1).

5.2 Segmentation results

5.2.1 RGB-D segmentation

We first analyze the performance of the proposed MixPrompt framework for RGB-D (depth) segmentation, comparing it with several state-of-the-art multimodal fusion methods. The results are summarized in Table 1, which reports the performance on the NYU Depth V2 and SUN-RGBD datasets.

On the NYU Depth V2 dataset, MixPrompt achieves the highest mIoU score of 61.2 with 87.2M parameters and 109.0G FLOPs computational cost, demonstrating the efficiency of our approach. In comparison, the second-best method, DPLNet, achieves an mIoU of 59.3 with slightly more parameters and lower FLOPs. Methods like ACNet and SGNet, with mIoUs of 48.3 and 51.1, respectively, perform significantly worse, highlighting the advantages of our MixPrompt.

On the SUN-RGBD dataset, MixPrompt again achieves the highest mIoU of 53.5, surpassing other methods by a notable margin. DPLNet ranks second with an mIoU of 52.8, while CMX-MiT-B5 follows closely with 52.4. Other methods, such as ACNet and SGNet, continue to show lower performance, with mIoUs of 48.1 and 48.6, respectively. The results on SUN-RGBD further reinforce the strength of MixPrompt. A key advantage of MixPrompt is its computational efficiency. With 87.2M parameters and 109.0G FLOPs on the NYU Depth V2 dataset, MixPrompt achieves competitive accuracy while being more lightweight compared to other high-performance models, such as CMX (MiT-B5). The efficient design of the MixPrompt framework, using a lightweight prompting module integrated with a pretrained RGB backbone, avoids the need for parallel networks or complex fusion architectures that typically increase both model size and computational cost. Another notable method is DFormer [26], which has significantly fewer parameters compared to other recent approaches. While its design of using a shared branch for both RGB and auxiliary modalities contributes to a parameter-efficient architecture, this shared parameterization also limits flexibility of the model. As a result, DFormer significantly underperforms in comparison to our framework.

To ensure the fairness of our experimental setup, we additionally examined the impact of different backbone pretraining settings. Specifically, we re-trained several representative multi-modal methods (e.g., CMX and CMNeXt) using the same ADE20K-pretrained weights as ours to provide an equitable

comparison. The results consistently show that while these models benefit slightly from stronger initialization, our method still achieves a clear advantage (around 2.9–3.1 mIoU higher on NYUDepth) with significantly fewer trainable parameters. Detailed experimental results and analysis are provided in the supplementary material (Section C.3).

5.2.2 RGB-T segmentation

We then analyze the performance of MixPrompt on the RGB-T (Thermal) segmentation dataset MFNet. The results, shown in Table 2, report both class-wise and overall mIoU.

On the overall mIoU metric, MixPrompt achieves the highest score of 60.1, outperforming all other models in the comparison. The second-best method, CMNeXt, achieves an mIoU of 59.9. These top performers are followed by other notable methods such as CMX (MiT-B4), which scored 59.7. In contrast, models like MFNet and RTFNet achieved significantly lower mIoUs of 39.7 and 53.2, respectively, showcasing the advantages of the MixPrompt framework. Focusing on the class-wise performance, our model performs exceptionally well on classes such as "Car" and "Bike", with scores of 90.2 and 74.5, respectively. These scores are higher than those achieved by the best-performing models, such as CMNeXt, which scored 91.5 and 75.3 for the same classes.

Notably, our model excels in the Car Top (CT) class, achieving an outstanding performance of 48.3, which surpasses all other models in this category.

Despite the competitive performance in many classes, our model continues to demonstrate an overall advantage, achieving a balance between class-wise accuracy and computational efficiency. With 87.2M parameters and 109.0G FLOPs, MixPrompt outperforms others with comparable or even fewer parameters, while maintaining strong class performance.

5.2.3 Other auxiliary modalities

The results in Table 3 compare different methods on the RGB-E (Event) and RGB-L (Lidar) segmentation tasks from the DELIVER dataset. For the RGB-E task, our model achieves a notable mIoU score of 58.0, surpassing all other RGB-E models, including the second-best CMNeXt and CMX, demonstrating the efficiency and effectiveness of our approach in handling multi-modal RGB-E data.

In the RGB-L task, our model further establishes its superiority by achieving the highest mIoU of 59.1. It outperforms the next best method by a considerable margin. Despite having only 29.9M parameters, our model delivers top-tier performance, demonstrating both efficiency and strong segmentation capabilities in the RGB-L setting.

Table 3: Comparison of RGB-Event and RGB-Lidar segmentation performance on the DELIVER dataset. The highest mIoU for each condition is highlighted in bold, while the second-best score is underlined.

Method	Modal	Backbone	Params	mIoU
HRFuser [46]	RGB	HRFormer-T	29.9M	48.0
CMNeXt [8]	RGB	MiT-B2	25.8M	57.2
HRFuser [46]	RGB-E	HRFormer-T	30.5M	42.2
TokenFus. [21]	RGB-E	MiT-B2	26.0M	45.6
CMX [7]	RGB-E	MiT-B2	66.6M	56.5
CMNeXt [8]	RGB-E	MiT-B2	58.7M	<u>57.5</u>
Ours	RGB-E	MiT-B2	29.9M	**58.0**
HRFuser [46]	RGB-L	HRFormer-T	30.5M	43.1
TokenFus. [21]	RGB-L	MiT-B2	26.0M	53.0
CMX [7]	RGB-L	MiT-B2	66.6M	56.4
CMNeXt [8]	RGB-L	MiT-B2	58.7M	<u>58.0</u>
Ours	RGB-L	MiT-B2	29.9M	**59.1**

Overall, our model consistently performs at the top across both RGB-E and RGB-L modalities, showing a robust ability to integrate and process multimodal data for segmentation tasks. The relatively low number of parameters required further emphasizes the efficiency of our approach compared to other high-performing models.

5.3 Ablation study

To comprehensively evaluate our approach, we conduct an ablation study on the NYU Depth V2 dataset using MiT-B5 as the default model. The ablations cover three main aspects: the effectiveness of each module, the detailed design choices within each module, and the impact of key hyperparameters.

5.3.1 Effectiveness of each module

In order to evaluate the contributions of the key components in our proposed method, we conduct an ablation study focusing on two essential modules: the pretrained prompt extractor and the mixed prompting module. The results are summarized in Table 4.

When both modules are enabled, the best performance, with an mIoU of 60.1%, is achieved. However, when the pretrained prompt extractor is disabled, where we employ a simple patch embedding layer to integrate the auxiliary modality, the model achieves an mIoU of 58.8%. Similarly, if the mixed prompting module is removed, modality fusion is achieved through direct addition of the features without any alignment, and the mIoU score decreases slightly to 59.5%. From these experiments, the combination of the pretrained prompt extractor and the mixed prompting module provides the best results, highlighting that both modules in our proposed framework play an important role in enhancing performance.

Table 4: Ablation results for the pretrained prompt extractor and the mixed prompting module.

Prompt extractor	Mixed Prompting	Trainable params	FLOPs	mIoU (%)
✓	✓	5.7M	109.0G	**60.1**
✗	✓	5.5M	104.7G	58.8
✓	✗	5.4M	108.7G	59.5

5.3.2 Prompt extractor

We further investigate the design of the pretrained prompt extractor, beginning with an analysis of whether initializing the extractor with pretrained weights affects performance. As shown in Table 5, using a randomly initialized ResNet50 prompt extractor results in an mIoU of 59.5%, whereas initializing it with pretrained weights improves performance to 60.1%. This highlights the effectiveness of leveraging pretrained RGB models for extracting initial prompts. The pretrained backbone enables the model to extract more meaningful representations from the auxiliary modality, ultimately leading to better segmentation results.

Table 5: Impact of initializing the ResNet50 prompt extractor with pretrained weights.

Initialization type	mIoU (%)
Random	59.5
Pretrained	**60.1**

Next, we assess the impact of different prompt extractor architectures, with the results presented in Table 6. Given that the backbone follows the MiT architecture, we first evaluate various MiT variants as the prompt extractor. The results from MiT-B1 show that deeper extractors lead to lower mIoU, while progressively reducing the depth improves performance, with the best result achieved using only the first stage. Notably, ResNet50 outperforms MiT-B1, highlighting the effectiveness of convolutional models in extracting initial prompts. Additionally, increasing the size of MiT extractors offers no further improvements, reinforcing the advantage of convolutional extractors.

Table 6: Impact of different prompt extractor architectures and the number of layers used. A shallower convolutional extractor focusing on early-stage features achieves the best results.

Prompt extractor	Layers	mIoU (%)
mit-b1	stage {1,2,3,4}	59.2
mit-b1	stage {1,2,3}	59.5
mit-b1	stage {1,2}	59.6
mit-b1	stage {1}	59.7
mit-b2	stage {1}	59.6
mit-b4	stage {1}	59.2
mit-b5	stage {1}	59.3
ResNet50	stage {1,2,3,4}	58.9
ResNet50	stage {1,2,3}	59.5
ResNet50	stage {1,2}	59.9
ResNet50	stage {1}	**60.1**

These findings suggest that a pretrained convolutional prompt extractor focusing on early-stage features is more beneficial for prompted segmentation. The first stage of a pretrained ResNet50 provides the best performance. Therefore, we adopt this configuration as our final design.

5.3.3 Prompt mixing

We further investigate the impact of different prompt mixing configurations, particularly the effect of multi-subspace prompt mixing when applied to either the RGB or auxiliary modality. The results are summarized in Table 7.

From the results, the model achieves an mIoU of 59.3% without multi-subspace mixing. When multi-subspace mixing is introduced to the RGB modality, performance improves significantly to 60.1%, demonstrating the benefit of refining RGB prompts through multi-subspace alignment. Conversely, applying multi-subspace mixing only to the auxiliary modality yields a smaller improvement, reaching 59.7%. Interestingly, enabling multi-subspace mixing for both modalities does not lead to further gains and instead results in a slightly lower mIoU of 59.8% compared to the RGB-only setting.

Table 7: Ablation study on multi-subspace prompt mixing. The best result is achieved when multi-subspace mixing is applied only to RGB prompts.

RGB mixing	Auxiliary mixing	mIoU (%)
✗	✗	59.3
✓	✗	**60.1**
✗	✓	59.7
✓	✓	59.8

These results suggest that enhancing the RGB modality with multi-subspace mixing plays a more crucial role in improving segmentation performance. In contrast, applying the same strategy to the auxiliary modality provides more limited benefits, and simultaneous application to both may introduce redundant or conflicting information. Thus, our final design prioritizes multi-subspace mixing for RGB prompts to achieve optimal results.

5.3.4 Hyperparameters

We further perform an ablation study on key hyperparameters. First, we analyze the effect of the rank downscale ratio $\frac{d}{r}$, which controls the intermediate feature dimension and effectively determines the rank of the low-rank subspace. A larger ratio corresponds to a smaller rank and fewer trainable parameters. As shown in Table 8, increasing the downscale ratio from 1 to 4 improves the mIoU from 59.4% to 60.1%, indicating that a moderate reduction in rank enhances feature efficiency. However, when the ratio is further increased to 8, performance drops slightly to 59.6%, suggesting that an excessively small rank may lead to information loss and hinder performance. The optimal trade-off is achieved at a ratio of 4.

Next, we investigate the impact of the number of subspaces n used for prompt mixing. Unlike the rank downscale ratio, this parameter does not affect parameter efficiency of the model. As reported in Table 9, increasing the number of subspaces from 1 to 4 progressively enhances performance, reaching a peak mIoU of 60.1%. However, further increasing the number of subspaces to 8 results in a performance decline, suggesting that overly complex prompt mixing may introduce unnecessary redundancy.

Furthermore, we validated our hyperparameter configuration on multiple multimodal datasets, including RGB-Thermal, RGB-LiDAR, and RGB-Event. The results indicate that the selected values strike an effective balance among model capacity, generalization, and computational efficiency. Due to space limitations, more detailed results are provided in the supplementary material (Section C.7).

Table 8: Ablation study on the rank downscale ratio.

Rank down scale ratio $\frac{d}{r}$	1	2	4	8
mIoU (%)	59.4	59.8	**60.1**	59.6

Table 9: Ablation study on the number of subspaces for prompt mixing.

Num. of Subspace n	1	2	4	8
mIoU (%)	59.3	59.8	**60.1**	59.3

6 Conclusion

In this paper, we introduced MixPrompt, a novel framework for multimodal semantic segmentation that efficiently integrates auxiliary modalities into pretrained RGB models through prompt tuning. By leveraging a lightweight prompting module and multi-subspace alignment, MixPrompt successfully enhances model performance while maintaining parameter efficiency. Our method addresses the challenges of increased model complexity and data scarcity commonly associated with multimodal segmentation tasks. Through comprehensive experiments on multiple datasets, including NYU Depth V2, SUN-RGBD, MFNet, and DELIVER, we demonstrated that MixPrompt outperforms existing dual-backbone approaches with fewer parameters, establishing it as a highly effective and scalable solution.

Acknowledgment

This work was supported by the Joint Funds of the National Natural Science Foundation of China (NSFC) (No. U2336211), the Major Research Plan of the NSFC (No. 92467206), and the NSFC Grant (No. 62576364).

References

[1] Marius Cordts, Mohamed Omran, Sebastian Ramos, Timo Rehfeld, Markus Enzweiler, Rodrigo Benenson, Uwe Franke, Stefan Roth, and Bernt Schiele. The cityscapes dataset for semantic urban scene understanding. In *Proceedings of the IEEE conference on computer vision and pattern recognition*, pages 3213–3223, 2016.

[2] Bolei Zhou, Hang Zhao, Xavier Puig, Sanja Fidler, Adela Barriuso, and Antonio Torralba. Scene parsing through ade20k dataset. In *Proceedings of the IEEE conference on computer vision and pattern recognition*, pages 633–641, 2017.

[3] Xinxin Hu, Kailun Yang, Lei Fei, and Kaiwei Wang. Acnet: Attention based network to exploit complementary features for rgbd semantic segmentation. In *2019 IEEE International conference on image processing (ICIP)*, pages 1440–1444. IEEE, 2019.

[4] Lin-Zhuo Chen, Zheng Lin, Ziqin Wang, Yong-Liang Yang, and Ming-Ming Cheng. Spatial information guided convolution for real-time rgbd semantic segmentation. *IEEE Transactions on Image Processing*, 30:2313–2324, 2021.

[5] Xiaokang Chen, Kwan-Yee Lin, Jingbo Wang, Wayne Wu, Chen Qian, Hongsheng Li, and Gang Zeng. Bi-directional cross-modality feature propagation with separation-and-aggregation gate for rgb-d semantic segmentation. In *European conference on computer vision*, pages 561–577. Springer, 2020.

[6] Yikai Wang, Wenbing Huang, Fuchun Sun, Tingyang Xu, Yu Rong, and Junzhou Huang. Deep multimodal fusion by channel exchanging. *Advances in neural information processing systems*, 33:4835–4845, 2020.

[7] Jiaming Zhang, Huayao Liu, Kailun Yang, Xinxin Hu, Ruiping Liu, and Rainer Stiefelhagen. Cmx: Cross-modal fusion for rgb-x semantic segmentation with transformers. *IEEE Transactions on Intelligent Transportation Systems*, 2023.

[8] Jiaming Zhang, Ruiping Liu, Hao Shi, Kailun Yang, Simon Reiß, Kunyu Peng, Haodong Fu, Kaiwei Wang, and Rainer Stiefelhagen. Delivering arbitrary-modal semantic segmentation. In *Proceedings of the IEEE/CVF Conference on Computer Vision and Pattern Recognition*, pages 1136–1147, 2023.

[9] Zhiwei Hao, Zhongyu Xiao, Yong Luo, Jianyuan Guo, Jing Wang, Li Shen, and Han Hu. Primkd: Primary modality guided multimodal fusion for rgb-d semantic segmentation. In *Proceedings of the 32nd ACM International Conference on Multimedia*, pages 1943–1951, 2024.

[10] Qishen Ha, Kohei Watanabe, Takumi Karasawa, Yoshitaka Ushiku, and Tatsuya Harada. Mfnet: Towards real-time semantic segmentation for autonomous vehicles with multi-spectral scenes. In *2017 IEEE/RSJ International Conference on Intelligent Robots and Systems (IROS)*, pages 5108–5115. IEEE, 2017.

[11] Yuxiang Sun, Weixun Zuo, and Ming Liu. Rtfnet: Rgb-thermal fusion network for semantic segmentation of urban scenes. *IEEE Robotics and Automation Letters*, 4(3):2576–2583, 2019.

[12] Shreyas S Shivakumar, Neil Rodrigues, Alex Zhou, Ian D Miller, Vijay Kumar, and Camillo J Taylor. Pst900: Rgb-thermal calibration, dataset and segmentation network. In *2020 IEEE international conference on robotics and automation (ICRA)*, pages 9441–9447. IEEE, 2020.

[13] Yuxiang Sun, Weixun Zuo, Peng Yun, Hengli Wang, and Ming Liu. Fuseseg: Semantic segmentation of urban scenes based on rgb and thermal data fusion. *IEEE Transactions on Automation Science and Engineering*, 18(3):1000–1011, 2020.

[14] Shaohua Dong, Yunhe Feng, Qing Yang, Yan Huang, Dongfang Liu, and Heng Fan. Efficient multimodal semantic segmentation via dual-prompt learning. *arXiv preprint arXiv:2312.00360*, 2023.

[15] Nathan Silberman, Derek Hoiem, Pushmeet Kohli, and Rob Fergus. Indoor segmentation and support inference from rgbd images. In *Computer Vision–ECCV 2012: 12th European Conference on Computer Vision, Florence, Italy, October 7-13, 2012, Proceedings, Part V 12*, pages 746–760. Springer, 2012.

[16] Haotian Liu, Chunyuan Li, Qingyang Wu, and Yong Jae Lee. Visual instruction tuning. *Advances in neural information processing systems*, 36, 2024.

[17] Gen Luo, Yiyi Zhou, Tianhe Ren, Shengxin Chen, Xiaoshuai Sun, and Rongrong Ji. Cheap and quick: Efficient vision-language instruction tuning for large language models. *Advances in Neural Information Processing Systems*, 36, 2024.

[18] Zhiwei Hao, Jianyuan Guo, Li Shen, Yong Luo, Han Hu, and Yonggang Wen. Adem-vl: Adaptive and embedded fusion for efficient vision-language tuning. *arXiv preprint arXiv:2410.17779*, 2024.

[19] Shuran Song, Samuel P Lichtenberg, and Jianxiong Xiao. Sun rgb-d: A rgb-d scene understanding benchmark suite. In *Proceedings of the IEEE conference on computer vision and pattern recognition*, pages 567–576, 2015.

[20] Zongwei WU, Zhuyun Zhou, Guillaume Allibert, Christophe Stolz, Cédric Demonceaux, and Chao Ma. Transformer fusion for indoor rgb-d semantic segmentation. *Available at SSRN 4251286*, 2022.

[21] Yikai Wang, Xinghao Chen, Lele Cao, Wenbing Huang, Fuchun Sun, and Yunhe Wang. Multimodal token fusion for vision transformers. In *Proceedings of the IEEE/CVF conference on computer vision and pattern recognition*, pages 12186–12195, 2022.

[22] Daniel Seichter, Mona Köhler, Benjamin Lewandowski, Tim Wengefeld, and Horst-Michael Gross. Efficient rgb-d semantic segmentation for indoor scene analysis. In *2021 IEEE international conference on robotics and automation (ICRA)*, pages 13525–13531. IEEE, 2021.

[23] Zhen Feng, Yanning Guo, and Yuxiang Sun. Cekd: Cross-modal edge-privileged knowledge distillation for semantic scene understanding using only thermal images. *IEEE Robotics and Automation Letters*, 8(4):2205–2212, 2023.

[24] Jinming Cao, Hanchao Leng, Dani Lischinski, Daniel Cohen-Or, Changhe Tu, and Yangyan Li. Shapeconv: Shape-aware convolutional layer for indoor rgb-d semantic segmentation. In *Proceedings of the IEEE/CVF international conference on computer vision*, pages 7088–7097, 2021.

[25] Rohit Girdhar, Mannat Singh, Nikhila Ravi, Laurens Van Der Maaten, Armand Joulin, and Ishan Misra. Omnivore: A single model for many visual modalities. In *Proceedings of the IEEE/CVF Conference on Computer Vision and Pattern Recognition*, pages 16102–16112, 2022.

[26] Bowen Yin, Xuying Zhang, Zhongyu Li, Li Liu, Ming-Ming Cheng, and Qibin Hou. Dformer: Rethinking rgbd representation learning for semantic segmentation. *arXiv preprint arXiv:2309.09668*, 2023.

[27] Alec Radford, Jong Wook Kim, Chris Hallacy, Aditya Ramesh, Gabriel Goh, Sandhini Agarwal, Girish Sastry, Amanda Askell, Pamela Mishkin, Jack Clark, et al. Learning transferable visual models from natural language supervision. In *International conference on machine learning*, pages 8748–8763. PMLR, 2021.

[28] Hyojin Bahng, Ali Jahanian, Swami Sankaranarayanan, and Phillip Isola. Exploring visual prompts for adapting large-scale models. *arXiv preprint arXiv:2203.17274*, 2022.

[29] Menglin Jia, Luming Tang, Bor-Chun Chen, Claire Cardie, Serge Belongie, Bharath Hariharan, and Ser-Nam Lim. Visual prompt tuning. In *European Conference on Computer Vision*, pages 709–727. Springer, 2022.

[30] Edward J Hu, Yelong Shen, Phillip Wallis, Zeyuan Allen-Zhu, Yuanzhi Li, Shean Wang, Lu Wang, and Weizhu Chen. Lora: Low-rank adaptation of large language models. *arXiv preprint arXiv:2106.09685*, 2021.

[31] Shihan Dou, Enyu Zhou, Yan Liu, Songyang Gao, Wei Shen, Limao Xiong, Yuhao Zhou, Xiao Wang, Zhiheng Xi, Xiaoran Fan, et al. Loramoe: Alleviating world knowledge forgetting in large language models via moe-style plugin. In *Proceedings of the 62nd Annual Meeting of the Association for Computational Linguistics (Volume 1: Long Papers)*, pages 1932–1945, 2024.

[32] Noam Shazeer, Azalia Mirhoseini, Krzysztof Maziarz, Andy Davis, Quoc Le, Geoffrey Hinton, and Jeff Dean. Outrageously large neural networks: The sparsely-gated mixture-of-experts layer. *arXiv preprint arXiv:1701.06538*, 2017.

[33] Xiaohan Ding, Xiangyu Zhang, Ningning Ma, Jungong Han, Guiguang Ding, and Jian Sun. Repvgg: Making vgg-style convnets great again. In *Proceedings of the IEEE/CVF conference on computer vision and pattern recognition*, pages 13733–13742, 2021.

[34] Enze Xie, Wenhai Wang, Zhiding Yu, Anima Anandkumar, Jose M Alvarez, and Ping Luo. Segformer: Simple and efficient design for semantic segmentation with transformers. *Advances in neural information processing systems*, 34:12077–12090, 2021.

[35] Kaiming He, Xiangyu Zhang, Shaoqing Ren, and Jian Sun. Deep residual learning for image recognition. In *Proceedings of the IEEE conference on computer vision and pattern recognition*, pages 770–778, 2016.

[36] Han Xu, Jiayi Ma, Junjun Jiang, Xiaojie Guo, and Haibin Ling. U2fusion: A unified unsupervised image fusion network. *IEEE Transactions on Pattern Analysis and Machine Intelligence*, 44(1):502–518, 2020.

[37] Jiangtao Xu, Kaige Lu, and Han Wang. Attention fusion network for multi-spectral semantic segmentation. *Pattern Recognition Letters*, 146:179–184, 2021.

[38] Qiang Zhang, Shenlu Zhao, Yongjiang Luo, Dingwen Zhang, Nianchang Huang, and Jungong Han. Abmdrnet: Adaptive-weighted bi-directional modality difference reduction network for rgb-t semantic segmentation. In *Proceedings of the IEEE/CVF Conference on Computer Vision and Pattern Recognition*, pages 2633–2642, 2021.

[39] Fuqin Deng, Hua Feng, Mingjian Liang, Hongmin Wang, Yong Yang, Yuan Gao, Junfeng Chen, Junjie Hu, Xiyue Guo, and Tin Lun Lam. Feanet: Feature-enhanced attention network for rgb-thermal real-time semantic segmentation. In *2021 IEEE/RSJ international conference on intelligent robots and systems (IROS)*, pages 4467–4473. IEEE, 2021.

[40] Wujie Zhou, Jinfu Liu, Jingsheng Lei, Lu Yu, and Jenq-Neng Hwang. Gmnet: Graded-feature multilabel-learning network for rgb-thermal urban scene semantic segmentation. *IEEE Transactions on Image Processing*, 30:7790–7802, 2021.

[41] Jinyuan Liu, Xin Fan, Zhanbo Huang, Guanyao Wu, Risheng Liu, Wei Zhong, and Zhongxuan Luo. Target-aware dual adversarial learning and a multi-scenario multi-modality benchmark to fuse infrared and visible for object detection. In *Proceedings of the IEEE/CVF conference on computer vision and pattern recognition*, pages 5802–5811, 2022.

[42] Mingjian Liang, Junjie Hu, Chenyu Bao, Hua Feng, Fuqin Deng, and Tin Lun Lam. Explicit attention-enhanced fusion for rgb-thermal perception tasks. *IEEE Robotics and Automation Letters*, 8(7):4060–4067, 2023.

[43] Wujie Zhou, Shaohua Dong, Meixin Fang, and Lu Yu. Cacfnet: Cross-modal attention cascaded fusion network for rgb-t urban scene parsing. *IEEE Transactions on Intelligent Vehicles*, 2023.

[44] Zhu Liu, Jinyuan Liu, Benzhuang Zhang, Long Ma, Xin Fan, and Risheng Liu. Paif: Perception-aware infrared-visible image fusion for attack-tolerant semantic segmentation. In *Proceedings of the 31st ACM International Conference on Multimedia*, pages 3706–3714, 2023.

[45] Jinyuan Liu, Zhu Liu, Guanyao Wu, Long Ma, Risheng Liu, Wei Zhong, Zhongxuan Luo, and Xin Fan. Multi-interactive feature learning and a full-time multi-modality benchmark for image fusion and segmentation. In *Proceedings of the IEEE/CVF international conference on computer vision*, pages 8115–8124, 2023.

[46] Tim Broedermann, Christos Sakaridis, Dengxin Dai, and Luc Van Gool. Hrfuser: A multi-resolution sensor fusion architecture for 2d object detection. In *2023 IEEE 26th International Conference on Intelligent Transportation Systems (ITSC)*, pages 4159–4166. IEEE, 2023.

[47] Nameirakpam Dhanachandra, Khumanthem Manglem, and Yambem Jina Chanu. Image segmentation using k-means clustering algorithm and subtractive clustering algorithm. *Procedia Computer Science*, 54:764–771, 2015.

[48] Ziwei Liu, Xiaoxiao Li, Ping Luo, Chen Change Loy, and Xiaoou Tang. Deep learning markov random field for semantic segmentation. *IEEE transactions on pattern analysis and machine intelligence*, 40(8):1814–1828, 2017.

[49] Raviteja Vemulapalli, Oncel Tuzel, Ming-Yu Liu, and Rama Chellapa. Gaussian conditional random field network for semantic segmentation. In *Proceedings of the IEEE conference on computer vision and pattern recognition*, pages 3224–3233, 2016.

[50] Jonathan Long, Evan Shelhamer, and Trevor Darrell. Fully convolutional networks for semantic segmentation. In *Proceedings of the IEEE conference on computer vision and pattern recognition*, pages 3431–3440, 2015.

[51] Di Lin, Yuanfeng Ji, Dani Lischinski, Daniel Cohen-Or, and Hui Huang. Multi-scale context intertwining for semantic segmentation. In *Proceedings of the European Conference on Computer Vision (ECCV)*, pages 603–619, 2018.

[52] Jun Fu, Jing Liu, Haijie Tian, Yong Li, Yongjun Bao, Zhiwei Fang, and Hanqing Lu. Dual attention network for scene segmentation. In *Proceedings of the IEEE/CVF conference on computer vision and pattern recognition*, pages 3146–3154, 2019.

[53] Yunchao Wei, Huaxin Xiao, Honghui Shi, Zequn Jie, Jiashi Feng, and Thomas S Huang. Revisiting dilated convolution: A simple approach for weakly-and semi-supervised semantic segmentation. In *Proceedings of the IEEE conference on computer vision and pattern recognition*, pages 7268–7277, 2018.

[54] Wen Huang, Hongbin Liu, Minxin Guo, and Neil Zhenqiang Gong. Visual hallucinations of multi-modal large language models. *arXiv preprint arXiv:2402.14683*, 2024.

[55] Dianmo Sheng, Dongdong Chen, Zhentao Tan, Qiankun Liu, Qi Chu, Jianmin Bao, Tao Gong, Bin Liu, Shengwei Xu, and Nenghai Yu. Towards more unified in-context visual understanding. In *Proceedings of the IEEE/CVF Conference on Computer Vision and Pattern Recognition*, pages 13362–13372, 2024.

[56] Léon Bottou. Stochastic gradient descent tricks. In *Neural Networks: Tricks of the Trade: Second Edition*, pages 421–436. Springer, 2012.

[57] Diederik P Kingma and Jimmy Ba. Adam: A method for stochastic optimization. *arXiv preprint arXiv:1412.6980*, 2014.

[58] Radhakrishnan Gopalapillai, Deepa Gupta, Mohammed Zakariah, and Yousef Ajami Alotaibi. Convolution-based encoding of depth images for transfer learning in rgb-d scene classification. *Sensors*, 21(23):7950, 2021.

[59] Tobias Pohlen, Alexander Hermans, Markus Mathias, and Bastian Leibe. Full-resolution residual networks for semantic segmentation in street scenes. In *Proceedings of the IEEE conference on computer vision and pattern recognition*, pages 4151–4160, 2017.

[60] Changqian Yu, Jingbo Wang, Chao Peng, Changxin Gao, Gang Yu, and Nong Sang. Learning a discriminative feature network for semantic segmentation. In *Proceedings of the IEEE conference on computer vision and pattern recognition*, pages 1857–1866, 2018.

[61] Changqian Yu, Jingbo Wang, Chao Peng, Changxin Gao, Gang Yu, and Nong Sang. Bisenet: Bilateral segmentation network for real-time semantic segmentation. In *Proceedings of the European conference on computer vision (ECCV)*, pages 325–341, 2018.

[62] Caner Hazirbas, Lingni Ma, Csaba Domokos, and Daniel Cremers. Fusenet: Incorporating depth into semantic segmentation via fusion-based cnn architecture. In *Computer Vision–ACCV 2016: 13th Asian Conference on Computer Vision, Taipei, Taiwan, November 20-24, 2016, Revised Selected Papers, Part I 13*, pages 213–228. Springer, 2017.

NeurIPS Paper Checklist

1. **Claims**

   Question: Do the main claims made in the abstract and introduction accurately reflect the paper's contributions and scope?

   Answer: [Yes]

   Justification: The abstract and introduction clearly summarize the three main contributions of this article.

   Guidelines:

   - The answer NA means that the abstract and introduction do not include the claims made in the paper.
   - The abstract and/or introduction should clearly state the claims made, including the contributions made in the paper and important assumptions and limitations. A No or NA answer to this question will not be perceived well by the reviewers.
   - The claims made should match theoretical and experimental results, and reflect how much the results can be expected to generalize to other settings.
   - It is fine to include aspirational goals as motivation as long as it is clear that these goals are not attained by the paper.

2. **Limitations**

   Question: Does the paper discuss the limitations of the work performed by the authors?

   Answer: [Yes]

   Justification: We discussed the limitations of our work in the supplementary materials.

   Guidelines:

   - The answer NA means that the paper has no limitation while the answer No means that the paper has limitations, but those are not discussed in the paper.
   - The authors are encouraged to create a separate "Limitations" section in their paper.
   - The paper should point out any strong assumptions and how robust the results are to violations of these assumptions (e.g., independence assumptions, noiseless settings, model well-specification, asymptotic approximations only holding locally). The authors should reflect on how these assumptions might be violated in practice and what the implications would be.
   - The authors should reflect on the scope of the claims made, e.g., if the approach was only tested on a few datasets or with a few runs. In general, empirical results often depend on implicit assumptions, which should be articulated.
   - The authors should reflect on the factors that influence the performance of the approach. For example, a facial recognition algorithm may perform poorly when image resolution is low or images are taken in low lighting. Or a speech-to-text system might not be used reliably to provide closed captions for online lectures because it fails to handle technical jargon.
   - The authors should discuss the computational efficiency of the proposed algorithms and how they scale with dataset size.
   - If applicable, the authors should discuss possible limitations of their approach to address problems of privacy and fairness.
   - While the authors might fear that complete honesty about limitations might be used by reviewers as grounds for rejection, a worse outcome might be that reviewers discover limitations that aren't acknowledged in the paper. The authors should use their best judgment and recognize that individual actions in favor of transparency play an important role in developing norms that preserve the integrity of the community. Reviewers will be specifically instructed to not penalize honesty concerning limitations.

3. **Theory assumptions and proofs**

   Question: For each theoretical result, does the paper provide the full set of assumptions and a complete (and correct) proof?

   Answer: [NA]

Justification: This paper does not include theoretical results.

Guidelines:

- The answer NA means that the paper does not include theoretical results.
- All the theorems, formulas, and proofs in the paper should be numbered and cross-referenced.
- All assumptions should be clearly stated or referenced in the statement of any theorems.
- The proofs can either appear in the main paper or the supplemental material, but if they appear in the supplemental material, the authors are encouraged to provide a short proof sketch to provide intuition.
- Inversely, any informal proof provided in the core of the paper should be complemented by formal proofs provided in appendix or supplemental material.
- Theorems and Lemmas that the proof relies upon should be properly referenced.

4. **Experimental result reproducibility**

   Question: Does the paper fully disclose all the information needed to reproduce the main experimental results of the paper to the extent that it affects the main claims and/or conclusions of the paper (regardless of whether the code and data are provided or not)?

   Answer: [Yes]

   Justification: We have disclosed all the information required for the main experimental results of the paper in the experimental section

   Guidelines:

   - The answer NA means that the paper does not include experiments.
   - If the paper includes experiments, a No answer to this question will not be perceived well by the reviewers: Making the paper reproducible is important, regardless of whether the code and data are provided or not.
   - If the contribution is a dataset and/or model, the authors should describe the steps taken to make their results reproducible or verifiable.
   - Depending on the contribution, reproducibility can be accomplished in various ways. For example, if the contribution is a novel architecture, describing the architecture fully might suffice, or if the contribution is a specific model and empirical evaluation, it may be necessary to either make it possible for others to replicate the model with the same dataset, or provide access to the model. In general. releasing code and data is often one good way to accomplish this, but reproducibility can also be provided via detailed instructions for how to replicate the results, access to a hosted model (e.g., in the case of a large language model), releasing of a model checkpoint, or other means that are appropriate to the research performed.
   - While NeurIPS does not require releasing code, the conference does require all submissions to provide some reasonable avenue for reproducibility, which may depend on the nature of the contribution. For example
     (a) If the contribution is primarily a new algorithm, the paper should make it clear how to reproduce that algorithm.
     (b) If the contribution is primarily a new model architecture, the paper should describe the architecture clearly and fully.
     (c) If the contribution is a new model (e.g., a large language model), then there should either be a way to access this model for reproducing the results or a way to reproduce the model (e.g., with an open-source dataset or instructions for how to construct the dataset).
     (d) We recognize that reproducibility may be tricky in some cases, in which case authors are welcome to describe the particular way they provide for reproducibility. In the case of closed-source models, it may be that access to the model is limited in some way (e.g., to registered users), but it should be possible for other researchers to have some path to reproducing or verifying the results.

5. **Open access to data and code**

   Question: Does the paper provide open access to the data and code, with sufficient instructions to faithfully reproduce the main experimental results, as described in supplemental material?

Answer: [Yes]

Justification: We will open source the code after the draft is finalized

Guidelines:

- The answer NA means that paper does not include experiments requiring code.
- Please see the NeurIPS code and data submission guidelines (`https://nips.cc/public/guides/CodeSubmissionPolicy`) for more details.
- While we encourage the release of code and data, we understand that this might not be possible, so "No" is an acceptable answer. Papers cannot be rejected simply for not including code, unless this is central to the contribution (e.g., for a new open-source benchmark).
- The instructions should contain the exact command and environment needed to run to reproduce the results. See the NeurIPS code and data submission guidelines (`https://nips.cc/public/guides/CodeSubmissionPolicy`) for more details.
- The authors should provide instructions on data access and preparation, including how to access the raw data, preprocessed data, intermediate data, and generated data, etc.
- The authors should provide scripts to reproduce all experimental results for the new proposed method and baselines. If only a subset of experiments are reproducible, they should state which ones are omitted from the script and why.
- At submission time, to preserve anonymity, the authors should release anonymized versions (if applicable).
- Providing as much information as possible in supplemental material (appended to the paper) is recommended, but including URLs to data and code is permitted.

6. **Experimental setting/details**

   Question: Does the paper specify all the training and test details (e.g., data splits, hyperparameters, how they were chosen, type of optimizer, etc.) necessary to understand the results?

   Answer: [Yes]

   Justification: We have detailed experimental instructions in the experimental section and supplementary materials.

   Guidelines:

   - The answer NA means that the paper does not include experiments.
   - The experimental setting should be presented in the core of the paper to a level of detail that is necessary to appreciate the results and make sense of them.
   - The full details can be provided either with the code, in appendix, or as supplemental material.

7. **Experiment statistical significance**

   Question: Does the paper report error bars suitably and correctly defined or other appropriate information about the statistical significance of the experiments?

   Answer: [Yes]

   Justification: All experimental results meet the requirements

   Guidelines:

   - The answer NA means that the paper does not include experiments.
   - The authors should answer "Yes" if the results are accompanied by error bars, confidence intervals, or statistical significance tests, at least for the experiments that support the main claims of the paper.
   - The factors of variability that the error bars are capturing should be clearly stated (for example, train/test split, initialization, random drawing of some parameter, or overall run with given experimental conditions).
   - The method for calculating the error bars should be explained (closed form formula, call to a library function, bootstrap, etc.)
   - The assumptions made should be given (e.g., Normally distributed errors).

- It should be clear whether the error bar is the standard deviation or the standard error of the mean.
- It is OK to report 1-sigma error bars, but one should state it. The authors should preferably report a 2-sigma error bar than state that they have a 96% CI, if the hypothesis of Normality of errors is not verified.
- For asymmetric distributions, the authors should be careful not to show in tables or figures symmetric error bars that would yield results that are out of range (e.g. negative error rates).
- If error bars are reported in tables or plots, The authors should explain in the text how they were calculated and reference the corresponding figures or tables in the text.

8. **Experiments compute resources**

   Question: For each experiment, does the paper provide sufficient information on the computer resources (type of compute workers, memory, time of execution) needed to reproduce the experiments?

   Answer: [Yes]

   Justification: We have relevant explanations in the supplementary materials.

   Guidelines:

   - The answer NA means that the paper does not include experiments.
   - The paper should indicate the type of compute workers CPU or GPU, internal cluster, or cloud provider, including relevant memory and storage.
   - The paper should provide the amount of compute required for each of the individual experimental runs as well as estimate the total compute.
   - The paper should disclose whether the full research project required more compute than the experiments reported in the paper (e.g., preliminary or failed experiments that didn't make it into the paper).

9. **Code of ethics**

   Question: Does the research conducted in the paper conform, in every respect, with the NeurIPS Code of Ethics `https://neurips.cc/public/EthicsGuidelines`?

   Answer: [Yes]

   Justification: Our research fully complies with the required ethical standards.

   Guidelines:

   - The answer NA means that the authors have not reviewed the NeurIPS Code of Ethics.
   - If the authors answer No, they should explain the special circumstances that require a deviation from the Code of Ethics.
   - The authors should make sure to preserve anonymity (e.g., if there is a special consideration due to laws or regulations in their jurisdiction).

10. **Broader impacts**

    Question: Does the paper discuss both potential positive societal impacts and negative societal impacts of the work performed?

    Answer: [Yes]

    Justification: We discuss the relevant impacts in the supplementary materials.

    Guidelines:

    - The answer NA means that there is no societal impact of the work performed.
    - If the authors answer NA or No, they should explain why their work has no societal impact or why the paper does not address societal impact.
    - Examples of negative societal impacts include potential malicious or unintended uses (e.g., disinformation, generating fake profiles, surveillance), fairness considerations (e.g., deployment of technologies that could make decisions that unfairly impact specific groups), privacy considerations, and security considerations.

- The conference expects that many papers will be foundational research and not tied to particular applications, let alone deployments. However, if there is a direct path to any negative applications, the authors should point it out. For example, it is legitimate to point out that an improvement in the quality of generative models could be used to generate deepfakes for disinformation. On the other hand, it is not needed to point out that a generic algorithm for optimizing neural networks could enable people to train models that generate Deepfakes faster.
- The authors should consider possible harms that could arise when the technology is being used as intended and functioning correctly, harms that could arise when the technology is being used as intended but gives incorrect results, and harms following from (intentional or unintentional) misuse of the technology.
- If there are negative societal impacts, the authors could also discuss possible mitigation strategies (e.g., gated release of models, providing defenses in addition to attacks, mechanisms for monitoring misuse, mechanisms to monitor how a system learns from feedback over time, improving the efficiency and accessibility of ML).

11. **Safeguards**

    Question: Does the paper describe safeguards that have been put in place for responsible release of data or models that have a high risk for misuse (e.g., pretrained language models, image generators, or scraped datasets)?

    Answer: [NA]

    Justification: There is no such risk in this paper.

    Guidelines:

    - The answer NA means that the paper poses no such risks.
    - Released models that have a high risk for misuse or dual-use should be released with necessary safeguards to allow for controlled use of the model, for example by requiring that users adhere to usage guidelines or restrictions to access the model or implementing safety filters.
    - Datasets that have been scraped from the Internet could pose safety risks. The authors should describe how they avoided releasing unsafe images.
    - We recognize that providing effective safeguards is challenging, and many papers do not require this, but we encourage authors to take this into account and make a best faith effort.

12. **Licenses for existing assets**

    Question: Are the creators or original owners of assets (e.g., code, data, models), used in the paper, properly credited and are the license and terms of use explicitly mentioned and properly respected?

    Answer: [Yes]

    Justification: This paper meets the relevant requirements.

    Guidelines:

    - The answer NA means that the paper does not use existing assets.
    - The authors should cite the original paper that produced the code package or dataset.
    - The authors should state which version of the asset is used and, if possible, include a URL.
    - The name of the license (e.g., CC-BY 4.0) should be included for each asset.
    - For scraped data from a particular source (e.g., website), the copyright and terms of service of that source should be provided.
    - If assets are released, the license, copyright information, and terms of use in the package should be provided. For popular datasets, `paperswithcode.com/datasets` has curated licenses for some datasets. Their licensing guide can help determine the license of a dataset.
    - For existing datasets that are re-packaged, both the original license and the license of the derived asset (if it has changed) should be provided.

- If this information is not available online, the authors are encouraged to reach out to the asset's creators.

13. **New assets**

    Question: Are new assets introduced in the paper well documented and is the documentation provided alongside the assets?

    Answer: [NA]

    Justification: This paper does not release new assets.

    Guidelines:

    - The answer NA means that the paper does not release new assets.
    - Researchers should communicate the details of the dataset/code/model as part of their submissions via structured templates. This includes details about training, license, limitations, etc.
    - The paper should discuss whether and how consent was obtained from people whose asset is used.
    - At submission time, remember to anonymize your assets (if applicable). You can either create an anonymized URL or include an anonymized zip file.

14. **Crowdsourcing and research with human subjects**

    Question: For crowdsourcing experiments and research with human subjects, does the paper include the full text of instructions given to participants and screenshots, if applicable, as well as details about compensation (if any)?

    Answer: [NA]

    Justification: The paper does not involve crowdsourcing nor research with human subjects.

    Guidelines:

    - The answer NA means that the paper does not involve crowdsourcing nor research with human subjects.
    - Including this information in the supplemental material is fine, but if the main contribution of the paper involves human subjects, then as much detail as possible should be included in the main paper.
    - According to the NeurIPS Code of Ethics, workers involved in data collection, curation, or other labor should be paid at least the minimum wage in the country of the data collector.

15. **Institutional review board (IRB) approvals or equivalent for research with human subjects**

    Question: Does the paper describe potential risks incurred by study participants, whether such risks were disclosed to the subjects, and whether Institutional Review Board (IRB) approvals (or an equivalent approval/review based on the requirements of your country or institution) were obtained?

    Answer: [NA]

    Justification: The paper does not involve crowdsourcing nor research with human subjects.

    Guidelines:

    - The answer NA means that the paper does not involve crowdsourcing nor research with human subjects.
    - Depending on the country in which research is conducted, IRB approval (or equivalent) may be required for any human subjects research. If you obtained IRB approval, you should clearly state this in the paper.
    - We recognize that the procedures for this may vary significantly between institutions and locations, and we expect authors to adhere to the NeurIPS Code of Ethics and the guidelines for their institution.
    - For initial submissions, do not include any information that would break anonymity (if applicable), such as the institution conducting the review.

16. **Declaration of LLM usage**

Question: Does the paper describe the usage of LLMs if it is an important, original, or non-standard component of the core methods in this research? Note that if the LLM is used only for writing, editing, or formatting purposes and does not impact the core methodology, scientific rigorousness, or originality of the research, declaration is not required.

Answer: [NA]

Justification: LLMs does not affect core methods, scientific rigor, or originality of research

Guidelines:

- The answer NA means that the core method development in this research does not involve LLMs as any important, original, or non-standard components.
- Please refer to our LLM policy (`https://neurips.cc/Conferences/2025/LLM`) for what should or should not be described.

A Related works

A.1 Semantic segmentation.

The task of semantic segmentation not only requires identifying objects within an image but also demands precise outlining of their boundaries, rendering them considerably more challenging compared to image classification tasks. The development of traditional methods can be divided into two major stages. The first stage revolves around classic approaches based on handcrafted features, ranging from k-means clustering [47] to Markov Random Fields [48] and Conditional Random Fields [49]. The second stage marks the shift to early deep learning-based methods, such as Fully Convolutional Networks [50], which laid the foundation for modern segmentation tasks. Building on this foundation, techniques like multi-scale pyramids [51], attention mechanisms [52], and dilated convolutions [53] have been introduced, significantly improving segmentation accuracy by capturing richer contextual information and enhancing feature representation.

Although these methods have achieved commendable performance, they typically rely on RGB images for predictions. However, RGB images alone often lack sufficient information for precise semantic segmentation, especially in complex scenarios such as low-light conditions, blurred textures, or occluded target objects. To address these challenges, researchers are exploring the integration of other data modalities, such as depth maps [15, 19] and Thermal images [10], leveraging the complementary advantages of multimodal data to enhance the accuracy and robustness of semantic segmentation across diverse environments.

Existing methods primarily focus on two aspects. The first aspect emphasizes the alignment and fusion between different modalities [3, 6, 20, 8, 21, 22, 10, 11, 13, 23]. Researchers explored diverse strategies for alignment and fusion across multiple levels, encompassing the input, intermediate feature extraction layers, and output. For instance, Cao *et al.* [24] incorporates geometric information from auxiliary modalities into convolutional weights, establishing a link between the weights and the underlying spatial relationships of corresponding pixels to better capture the spatial structure of scenes. Similarly, Hu *et al.* [3] introduces an additional attention-based auxiliary module to fuse features from different modalities, further balancing feature distributions and enabling the network to focus more effectively on the most relevant regions of the image. Zhang *et al.* [7] proposes innovative cross-modal feature calibration and fusion modules, aligning and calibrating feature differences in spatial and channel dimensions across modalities at multiple scales of the model.The second aspect focuses on more effective feature extraction [24, 5, 4, 25, 26]. For example, Girdhar *et al.* [25] introduces a novel Transformer architecture that is jointly pre-trained on images, videos, and single-view 3D data, equipping the model with cross-modal semantic feature extraction capabilities and making it suitable for downstream tasks across different modalities. Meanwhile, Zhang *et al.* [26] constructs a new large-scale RGB-D image dataset for pre-training, enhancing the ability of the model to encode both RGB and depth images.

Nevertheless, the introduction of additional modality-specific feature extraction networks significantly increases model complexity, resulting in an overwhelming training overhead. Moreover, the scarcity of existing multimodal datasets makes it challenging to support large-scale pretraining tasks, which hinders the model ability to be quickly fine-tuned for various downstream tasks across different modalities.

A.2 Multimodal Prompting.

Vision-Language Models (VLMs) are deep learning models that integrate both visual and textual information, with visual capabilities that enable understanding and reasoning across complex multimodal tasks. The introduction of visual prompts, complementing textual prompts, enables more granular, pixel-level instructions on multimodal inputs, helping to mitigate challenges in traditional multimodal language models, such as visual hallucinations [54] and linguistic biases [55]. For instance, CLIP [27] leverages contrastive learning to align shared semantic spaces between images and text. LLaVA [16], by combining visual prompts with large-scale pretrained language models, has achieved remarkable results in image-text reasoning and generation tasks. This approach not only taps into the powerful foundational capabilities of large-scale pretrained models but also allows visual prompts to adaptively establish connections between different modalities in various forms tailored to specific tasks. An initial attempt to apply prompt tuning to the multimodal semantic segmentation task was made by Dong *et al.* [14]. However, their approach utilizes the same summation operation

to fuse features from different modalities without considering the differences between the additional modality and the RGB modality, which may interfere with the feature distribution of the primary RGB modality and affect ability of the model to capture important visual information.

B Methodology Details

B.1 Details of mixed prompting

The detailed algorithmic procedure for the mixed prompting module is presented in Algorithm 1.

Algorithm 1 Mixed Prompting Module

Require: hidden state h_{i-1}, prompt e_{i-1}, low-rank matrices $W_{\text{rgb}} \in \mathbb{R}^{r \times d}$, $W_{\text{x}} \in \mathbb{R}^{r \times d}$, $W_{\text{up}} \in \mathbb{R}^{d \times r}$, number of subspaces n, mixing matrix $M \in \mathbb{R}^{n \times n}$, model layer L_i
Ensure: hidden state h_i, prompt e_i

$\hat{e}_{i-1} \leftarrow W_{\text{x}} e_{i-1}$
$\hat{h}_{i-1} \leftarrow W_{\text{rgb}} h_{i-1}$
$\hat{h}_{i-1} \leftarrow \text{reshape}(\hat{h}_{i-1}, (-1, n))$
$\hat{h}_{i-1} \leftarrow \hat{h}_{i-1} M$ ▷ *Mixing*
$\hat{h}_{i-1} \leftarrow \text{flatten}(\hat{h}_{i-1})$
$e_i \leftarrow W_{\text{up}}(\hat{e}_{i-1} + \hat{h}_{i-1})$ ▷ *new prompt*
$h_i \leftarrow L_i(h_{i-1} + e_i)$ ▷ *new hidden state*

C Additional Experiment Details.

C.1 Optimization and Schedule.

We provide detailed configurations for training on datasets including NYU Depth V2 [15], SUN-RGBD [19], MFNet [10], and DELIVER [8] datasets. The specific hyperparameters are summarized in Table 10.

For the *NYU Depth V2* dataset, we use SGD [56] with a weight decay of 5×10^{-4} and an initial learning rate of 0.04. The model is trained for 500 epochs with a batch size of 8. For the *SUN-RGBD* dataset, we adopt the AdamW optimizer [57] with 100 epochs and an initial learning rate of 0.005. For the *MFNet* dataset, we train for 500 epochs with the AdamW optimizer, a learning rate of 6×10^{-4}, and a batch size of 4. For the *DELIVER* dataset, we train for 200 epochs with a batch size of 2, using a learning rate of 6×10^{-5} and a weight decay factor of 0.01. All experiments are conducted on NVIDIA GeForce RTX 3090 GPUs. Data augmentation techniques, including random flipping, random cropping, and multiscale inference with scales {0.5, 0.75, 1.0, 1.25, 1.5, 1.75}, are applied during training for all datasets.

Table 10: Training configurations for different datasets. LR: Learning Rate, WD: Weight Decay, Mom: Momentum.

Dataset	Input Size	Batch Size	Epochs	Optimizer	LR	WD	Mom
NYUD-v2	480×640	8	500	SGD	4e-2	0.0005	0.9
SUN-RGBD	530×730	4	100	AdamW	5e-3	0.01	(0.9, 0.999)
MFNet	480×640	4	500	AdamW	6e-4	0.01	(0.9, 0.999)
DELIVER	1024×1024	2	200	AdamW	6e-5	0.01	(0.9, 0.999)

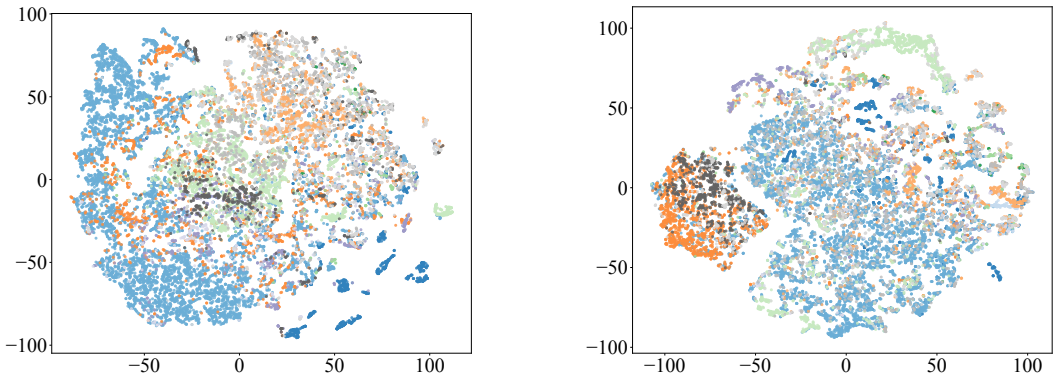

(a) RGB. (b) Depth.

Figure 4: t-SNE visualization of feature embeddings for RGB and depth inputs, indicating that the feature from depth images results in similar clustering levels to those from RGB images.

C.2 Analysis for Prompt Initialization

To further validate the feasibility of using pre-trained RGB models for prompt initialization, we conduct a t-SNE analysis to visualize the distribution of features extracted from both modalities.

In this analysis, each pixel is treated as a data point, and the corresponding ground truth serves as the label. The results, presented in Figure 4, demonstrate that **the feature representations for both RGB and depth inputs form clusters at a similar level in the lower-dimensional space**. For the RGB modality, the points are spread out with multiple clusters, reflecting the rich variety of information captured from the RGB image. Similarly, in the depth modality, the points also form well-defined clusters. This suggests that the features extracted from the depth modality, although distinct from RGB features in some aspects, are sufficiently informative, indicating that pretrained RGB models allows MixPrompt to efficiently integrate auxiliary modalities without requiring additional, modality-specific pretrained extractors.

C.3 Analysis for Different Backbone Pretraining Settings

This note addresses the concerns raised regarding the fairness of the experimental setup. To ensure a equitable comparison, we have conducted additional experiments where we initialized several prior multi-modal approaches (e.g., CMX and CMNeXt) with ADE20K-pretrained weights, followed by training on the NYUDepth dataset. The results are summarized below.

Table 11: Comparison of different method with different backbone pretraining settings.

Method	Backbone Pretraining	Trainable Params	mIoU (%)
Segformer	MiT-B5 (ADE20K)	82.7M	54.7
CMX	MiT-B5 (ImageNet)	181.1M	56.9
CMX	MiT-B5 (ADE20K)	181.1M	58.1
CMNeXt	MiT-B4 (ImageNet)	119.6M	56.9
CMNeXt	MiT-B4 (ADE20K)	119.6M	58.3
Ours	MiT-B5 (ADE20K)	**5.7M**	**61.2**

As shown in Table 11, we observe that CMX and CMNeXt do benefit from using the same strong baseline as ours, resulting in limited performance gains. However, the gap between their results and ours remains substantial (e.g., a 2.9–3.1 mIoU difference on the NYUDepth dataset). This comparison under the same pretrained setting demonstrates the effectiveness of our method over other multi-modal fusion approaches. Notably, our model achieves this with only 5.7M trainable parameters—significantly fewer than the alternatives.

Additionally, we conducted experiments where the single-modality RGB backbone (SegFormer) was also initialized with ADE20K-pretrained weights. The results further indicate that the performance

gains achieved by our method go well beyond what can be attributed to pretraining alone, highlighting the strength of our fusion strategy.

Overall, these experiments provide meaningful evidence for our fairness of the experimental setup.

C.4 Experiments on the Effectiveness of the Encoding Strategy

To evaluate the contribution of reusing the early layers of a pretrained RGB backbone as an embedding strategy for auxiliary modalities, we conducted additional experiments by replacing our pretrained RGB backbone with the convolution-based encoder proposed in [58]. Experiments were performed on both RGB-D and RGB-T datasets, and the results are summarized in Table 12.

Table 12: Comparison of different encoding methods in the Mixed Prompting Module.

Encoder Method	**NYUDepth (RGB-D)**	**MFNet (RGB-T)**
Convolution-Based Encoding [58]	58.7	56.8
Ours	**61.2**	**60.1**

As shown in Table 12, the previous convolution-based depth encoder does not adapt well to the prompting framework. It likely provides suboptimal prompt initialization, leading to an approximate performance drop of 2.5% mIoU compared to our trainable backbone on RGB-D datasets. Moreover, results on the RGB-T dataset reveal that it fails to generalize effectively to arbitrary modality encoders, limiting its scalability.

C.5 Quantitative Analysis of multi-subspace distributions.

To quantitatively characterize the diversity among the learned subspaces, we conducted additional analysis. Following the hierarchical encoder architecture of SegFormer, our backbone extracts four-stage multi-scale features with progressively lower spatial resolutions, denoted as d1-d4 (from highest to lowest resolution). For each stage, we compute the average pairwise cosine similarity between projected RGB subspace features, where values range from -1 (completely dissimilar) to 1 (identical). Lower (more negative) similarity values indicate greater diversity across subspaces. The "Avg.Sim (overall)" column summarizes the mean similarity across all four stages, providing an overall measure of inter-subspace diversity.

Table 13: Average pairwise cosine similarity (Sim) between RGB subspace features across different numbers of subspaces (n) and corresponding segmentation performance.

n	**Sim (d1)**	**Sim (d2)**	**Sim (d3)**	**Sim (d4)**	**Sim (overall)**	**mIoU (%)**
1	N/A	N/A	N/A	N/A	N/A	59.3
2	-0.0338	-0.0355	-0.0508	-0.0853	-0.0514	59.8
4	-0.1434	-0.1715	-0.2031	-0.2506	-0.1922	60.1
8	-0.0135	-0.0046	-0.0175	-0.0321	-0.0169	59.6

As reported in Table 13, we evaluated how varying the number of subspaces (n) affects feature diversity using RGB-D inputs from the NYU Depth V2 test set. Our analysis reveals that within the same n, similarity values become increasingly negative from high-resolution (d1) to low-resolution (d4) features. This occurs because high-resolution features predominantly capture modality-agnostic local patterns (e.g., edges and textures) that remain relatively consistent across subspaces, whereas lower-resolution features encode more abstract, global, and cross-modal semantics. Consequently, our multi-subspace prompt mixing more effectively disentangles these higher-level representations, resulting in greater divergence at coarser scales.

Furthermore, increasing n from 1 to 4 substantially reduces overall similarity (from -0.0514 to -0.1922), reflecting enhanced structural diversity that correlates with optimal segmentation performance (mIoU of 60.1%). However, further increasing n to 8 causes similarity magnitude to decrease (from -0.1922 to -0.0169), indicating over-fragmentation that diminishes subspace diversity and aligns with the observed performance degradation.

These quantitative results validate the core motivation behind our multi-subspace design: by introducing structural diversity and encouraging disentangled prompt composition, it effectively improves segmentation outcomes. While comprehensive visualizations of subspace distributions would provide additional intuitive insights, we believe this detailed statistical characterization offers compelling evidence for the effectiveness of our approach.

C.6 Analysis for Merging Strategy in the Mixed Prompting Module

We adopt a simple summation of the two prompt embeddings (h_{i-1} and e_{i-1}), primarily due to its parameter-efficiency and empirical effectiveness in our preliminary experiments. While our current approach is effective, we fully recognize the potential of alternative fusion strategies—such as concatenation followed by a projection layer, learnable weighted summation via gating, or attention-based fusion—to enable more expressive cross-modal interactions, as the reviewer rightly pointed out. However, these methods typically introduce additional parameters and computational overhead, potentially undermining the objective of preserving a compact and efficient prompting module, while also increasing the complexity of training.

To futher investigate the effectiveness of these fusion methods, we conducted ablation studies on different prompt fusion strategies using the NYUDepth dataset. The quantitative results are shown in the table below, and the implementation details of each variant are described as Table 14.

Concatenation. Concatenate h_{i-1} and e_{i-1} along the module dimension, and apply a linear transformation to fuse the combined representation back into the original embedding space.

Learnable Weighted Summation. Introduce a learnable gating vector $g \in \mathbb{R}^C$ and compute the fused prompt as $\sigma(g) \cdot h_{i-1} + (1 - \sigma(g)) \cdot e_{i-1}$, where σ denotes the sigmoid activation function. The gate g is initialized as a trainable parameter and applied channel-wise to adaptively modulate the contribution of each modality.

Attention Fusion. The fused prompt is obtained by computing cross-modal attention between e_{i-1} and h_{i-1} : $\mathrm{Attn}(Q, K, V) = \mathrm{softmax}\left(\frac{QK^\intercal}{\sqrt{d}}\right)V$.

Overall, our results on NYUDepth indicate that simple summation achieves the best performance among the evaluated strategies, highlighting its effectiveness as a lightweight and robust fusion mechanism. Although concatenation and learnable weighted summation offer more flexible interactions between the two prompt streams, they do not yield noticeable performance improvements in our setting. One possible explanation is that the two prompts already provide sufficiently complementary information, and more complex merging may introduce redundancy or disrupt this balance.In contrast, attention fusion not only degrades performance, but also incurs substantial memory overhead. This is primarily due to the pairwise similarity computation between all token positions, which generates a large $N \times N$ attention map, where N corresponds to the number of spatial positions in the feature map. For high-resolution inputs, N can be large, making this step particularly memory-intensive.

These findings collectively support our use of simple summation as a practical and efficient fusion strategy in the mixed prompting module. We believe these findings provide a useful reference for future work exploring more adaptive fusion mechanisms in multimodal prompting.

Table 14: Comparison of different prompt fusion strategies in the Mixed Prompting Module.

Fusion Method	Trainable params	FLOPs	mIoU (%)
Summation	5.74M	109.01G	**60.1**
Concatenation	5.83M	109.09G	59.4
Learnable Weighted Sum	5.74M	109.01G	59.5
Attention Fusion	5.84M	109.09G	57.0

C.7 Further Validation of Hyperparameter Selection Generalizability

To evaluate the generalizability of our selected settings (e.g., a rank downscale ratio of 4 and 4 subspaces), we conducted additional ablation studies on multiple datasets beyond the NYU Depth v2 dataset originally reported. Specifically, we evaluated the effect of these parameters on MFNet and DELIVER datasets, which encompass RGB-Thermal, RGB-LiDAR, and RGB-Event modalities.

These datasets represent diverse sensing conditions and semantic distributions, offering a broader testing ground for robustness.

Across the diverse datasets evaluated, our selected parameter configuration consistently demonstrated competitive performance and stable optimization behavior. These results indicate that our chosen values strike a favorable balance among model capacity, generalization, and computational efficiency, making them a practical default for a wide range of multimodal segmentation scenarios.

While slight tuning may still benefit extremely domain-shifted settings, our results demonstrate that the chosen configuration is robust and transferable, reducing the burden of per-dataset hyperparameter adjustment in practice.

Table 15: Ablation study on the Ratio (rank downscale ratio).

Dataset	Modal	Ratio=1	Ratio=2	Ratio=4	Ratio=8
NYU Depth v2	RGB-D	59.4	59.8	**60.1**	59.6
MFNet	RGB-T	58.8	59.2	**60.1**	59.7
DELIVER	RGB-L	57.6	58.0	**59.1**	58.4
DELIVER	RGB-E	57.2	57.8	**58.0**	57.8

Table 16: Ablation study on the Num (number of subspaces for prompt mixing)

Dataset	Modal	Num=1	Num=2	Num=4	Num=8
NYU Depth v2	RGB-D	59.3	59.8	**60.1**	59.3
MFNet	RGB-T	58.4	58.9	**60.1**	59.5
DELIVER	RGB-L	58.3	58.5	**59.1**	58.8
DELIVER	RGB-E	57.1	57.6	**58.0**	57.5

C.8 Experiments for Different Illumination Conditions

To validate the robustness of our method under varying illumination conditions, we report the performance on the RGB-T MFNet dataset under both daytime and nighttime conditions in Table 17.

On the daytime mIoU, our method achieves an mIoU score of 51.8, ranking second after the best-performing model, CMX (MiT-B4), which scores 52.5. In the nighttime mIoU, a standout performance is achieved, where our model achieves the highest score of 61.0, surpassing all other methods. This demonstrates superior ability of our method to segment objects under nighttime conditions, where challenges such as poor lighting and low visibility are most pronounced.

Table 17: Comparison of RGB-T segmentation performance on the MFNet dataset across daytime and nighttime conditions. The highest mIoU for each condition is highlighted in bold, while the second-best score is underlined.

Method	Modal	Day	Night
FRRN [59]	RGB	40.0	37.3
DFN [60]	RGB	38.0	42.3
BiSeNet [61]	RGB	44.8	47.7
SegFormer-B2 [34]	RGB	48.6	49.2
SegFormer-B4 [34]	RGB	49.4	52.4
MFNet [10]	RGB-T	36.1	36.8
FuseNet [62]	RGB-T	41.0	43.9
RTFNet [11]	RGB-T	45.8	54.8
FuseSeg [13]	RGB-T	47.8	54.6
GMNet [40]	RGB-T	49.0	57.7
CMX(MiT-B2) [7]	RGB-T	51.3	57.8
CMX(MiT-B4) [7]	RGB-T	**52.5**	59.4
CMNeXt [8]	RGB-T	50.5	<u>59.8</u>
Ours	RGB-T	<u>51.8</u>	**61.0**

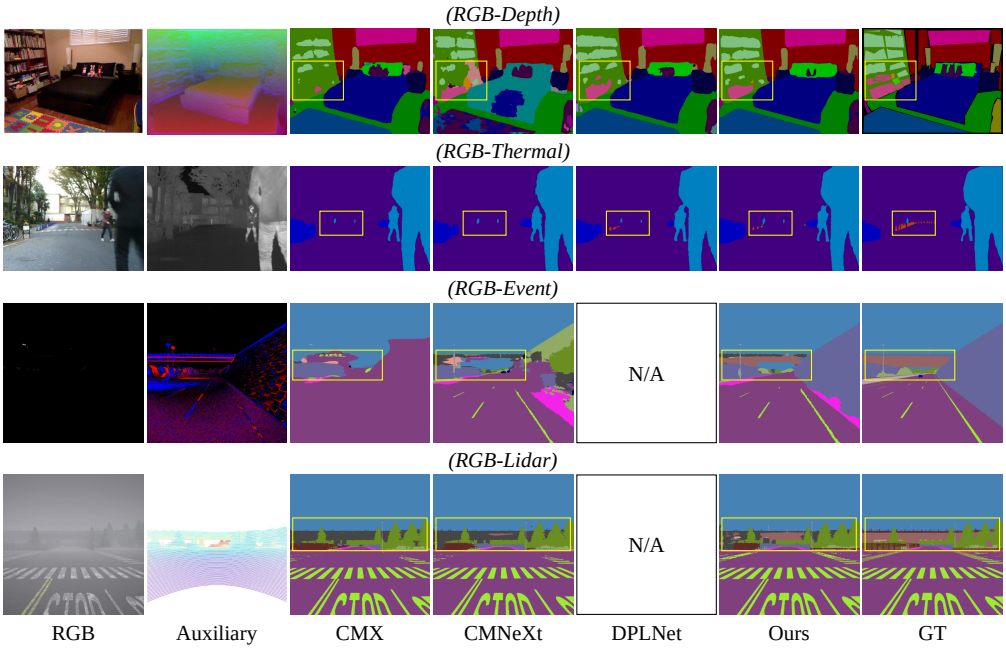

Figure 5: Visualization of results on the DELIVER dataset under depth, thermal, Event, and Lidar auxiliary modalities. DPLNet is not implemented for RGB-Event and RGB-Lidar data in the original paper.

C.9 Visualization

To provide a qualitative comparison between our MixPrompt method and existing approaches, we present visualizations of segmentation results from a sample image in each dataset used above. These visualizations are shown in Figure 5.

The comparison illustrates the ability of our model to produce more accurate and refined segmentation boundaries across a variety of auxiliary modalities, including depth, thermal, Event, and Lidar. Overall, the visual comparisons demonstrate the effectiveness of our multimodal fusion framework in generating high-quality segmentation outputs.

D Others

D.1 Social Impact Analysis

Our proposed multimodal fusion method can deploy artificial intelligence more widely in resource constrained environments such as agricultural robots or low-power edge devices, potentially reducing computational costs. However, the dependence on the pre training RGB backbone may inherit the deviation of training data, and the simplified architecture needs strict security verification before being deployed to key applications such as autonomous vehicle. We encourage responsible use and conduct additional fairness and robustness testing.

D.2 Limitation

Our current work is confined to the image multimodal domain and requires strictly aligned RGB-auxiliary data pairs. The exploration into other multimodal scenarios, such as weakly supervised or unpaired learning tasks is still limited. Addressing these limitations will become the basis of our future research.